ISSN Print: 2394-7500
ISSN Online: 2394-5869
Impact Factor: 5.2
IJAR 2016; 2(4): 543-552
www.allresearchjournal.com
Received: 27-02-2016
Accepted: 24-03-2016

G Alagumuthu
PG & Research,
Department of Chemistry,
Sri Paramakalyani College,
Alwarkurichi – 627412,
Tirunelveli District,
Tamilnadu, India.

T Anantha kumar
PG & Research,
Department of Chemistry,
Sri Paramakalyani College,
Alwarkurichi – 627412,
Tirunelveli District,
Tamilnadu, India.

M Kandasamy
PG & Research,
Department of Chemistry,
Sri Paramakalyani College,
Alwarkurichi – 627412,
Tirunelveli District,
Tamilnadu, India.

Correspondence
G Alagumuthu
PG & Research,
Department of Chemistry,
Sri Paramakalyani College,
Alwarkurichi – 627412,
Tirunelveli District,
Tamilnadu, India.

Synthesis, characterization and defluoridation study on modified biopolymers/TiO_2 nanocomposites

G Alagumuthu, T Anantha kumar, M Kandasamy

Abstract
The development of rapid and reliable processes for the synthesis of nanomaterials is of great importance in the field of nanotechnology. In this paper, the modified forms of chitosan beads such as carboxylated cross-linked chitosan beads (CCB), Grafted cross-linked chitosan beads (GCB) and Protonated cross-linked chitosan beads (PCB) were prepared synthetically from chitosan beads by chemical method. The synthesis of modified chitosan beads/TiO_2 nanocomposites was carried out by using LPD (Liquid Phase Deposition) technology in aqueous medium. The method was performed by mixing the modified chitosan beads with TiO_2 in the presence of PVA has been used as the capping agent. The synthesized nanocomposites were characterized by XRD, SEM with EDAX and UV-vis absorption spectroscopy. The present study was conducted to evaluate the feasibility of modified chitosan beads/TiO_2 nanocomposites for fluoride adsorption from aqueous solution. The residual adsorbents were also characterized by using XRD and SEM with EDAX analysis. A batch adsorption study was performed with function of contact time.

Keywords: Nanocomposites, Chitosan, Fluoride, Beads, Adsorption and Nanomaterials.

1. Introduction
Over the years groundwater has been regarded as the safest and most protected source of water, fit for drinking without treatment. There is a modest consideration given to the risks of chemical pollution, particularly to the presence of elevated levels of fluoride, arsenic and nitrate in groundwater. Recent studies, however, show the alarming threat of groundwater contaminations and the urgent need to find a low-cost treatment process for hazardous elements prior to drinking in different regions of the world. Specifically in the case of fluoride ions, consumption of water having excess fluoride over a prolonged period leads to a chronic disease known as fluorosis [1-4]. Fluoride in drinking water may be beneficial as well as detrimental depending upon its concentration [5]. When present in the significant amount it is considered as essential component for normal mineralization of bones, formation of dental enamel and prevention of dental carries [6]. Beyond the permissible limit (1–1.5 mg/L) it causes various disorders and diseases such as crippling, skeletal fluorosis, brittle bones, lung and bladder cancer, infertility in women, brain and hepatic damage and Alzheimer syndrome [7–9]. To prevent fluoride related diseases the exposed population has to be provided with safe drinking water.
Several methods have been suggested for removing excessive fluoride in water and they are chemical precipitation [10-11], ion exchange [12-13], adsorption [14-16] and electrolysis [17]. Among the methods reported adsorption seems to be the most attractive and selective technique for fluoride removal. Adsorption is still widely accepted pollution removal technique due to its ease of operation and cost effectiveness [18-20]. Researchers have used different types of adsorbents such as fired clay, brick powder, cotton cellulose, spent bleaching earth, activated carbon, zeolite, red mud, quick lime, silica, polymer, etc. [21-23]. Fluorine being a highly electronegative element has extraordinary tendency to get attracted by positively charged ions like aluminum and alkali metals [24] so, alumina is frequently used for the removal of fluoride from water [23, 25].
Chitosan is a cationic aminopolysaccharide copolymer of glucosamine and N-acetyl glucosamine, obtained by partial deacetylation of chitin, which originates from shells of crustaceans such as crabs and prawns [26]. Chitin and chitosan have varied potential applications in the areas of biotechnology, biomedicine and food ingredients [27-29].

In addition chitin and chitosan appear to be more useful biopolymers reported for the high potential of sorption of metal ions [30–32]. Chitosan is biodegradable, biocompatible and non-toxic biopolymer, reported to be an efficient heavy metal scavenger due to the presence of amino group [33]. The selectivity of the sorption is improved through chemical modification techniques based on protonation, carboxylation and grafting. In this work, we have attempted to synthesize a nanocomposite and used it as an adsorbent for the removal of fluoride from aqueous media. The main objective of the this paper is a systematic evaluation of the performance of a novel, synthesis of modified chitosan beads/TiO_2 nanocomposites for the uptake of fluoride from water and establish the probable mechanism of fluoride sorption.

2. Materials and methods

2.1. Materials

Chitosan with its deacetylation degree of 85% was supplied by Pelican Biotech and Chemicals Labs, Kerala (India). The viscosity of the chitosan solution was determined to be 700 mPas by Brookfield Dial Reading Viscometer using electronic drive-RVT model (USA make). The chitosan solution was maintained at a constant viscosity for beads preparation in order to maintain uniform molecular weight. NaOH, HCl, glacial acetic acid, glutaraldehyde, chloroacetic acid, Ethylenediamine and all other chemicals and reagents were of analytical grade.

2.2. Preparation of cross-linked chitosan beads (CB):

Chitosan (20 g) was dissolved in 2.0% glacial acetic acid solution (1000 ml). The chitosan solution was dropped into a 0.5M aqueous NaOH solution to form uniform chitosan beads. After gelling for a minimum of 16 h in 0.5M NaOH solution, the beads were washed with distilled water to a neutral pH. The wet beads were cross-linked with 2.5 wt.% glutaraldehyde solution and the ratio of glutaraldehyde to chitosan beads was approximately 1.5 ml/g of wet beads [34]. Cross-linking reaction occurred for 48 h and then cross-linked beads were washed with distilled water to remove any free glutaraldehyde.

2.3. Preparation of protonated cross-linked chitosan beads (PCB):

PCB was prepared in order to effectively utilize the amino groups of cross-linked chitosan beads for fluoride sorption. The cross-linked chitosan beads were treated with concentrated HCl for 30 min for protonation of beads [35]. The PCB was washed with distilled water to neutral pH, dried at room temperature and used for sorption studies [36].

2.4. Preparation of carboxylated cross-linked chitosan beads (CCB):

CCB was prepared in order to effectively utilize the hydroxyl groups of cross-linked chitosan beads for metal sorption. The crosslinked crosslinked chitosan beads were treated with aqueous 0.5M chloroacetic acid maintained at pH 8.0 using 0.1M NaOH for 10 h at room temperature to convert the hydroxyl groups to carboxyl groups. CCB was washed with distilled water to neutral pH, dried at room temperature and used for sorption studies [37].

2.5. Preparation of grafted cross-linked chitosan beads (GCB):

The wet cross-linked chitosan beads were treated with aqueous 0.5M chloroacetic acid maintained at pH 8.0 using 1.0M NaOH for 10 h at room temperature and then the reacted chitosan beads were washed with distilled water several times to remove unreacted reagents. In the second step, the carboxylated chitosan beads obtained through first reaction were treated in 100 ml of 1.0M ethylenediamine. Reaction was carried out for 5 h and the final chitosan beads were thoroughly washed using distilled water for several times and treated with concentrated HCl for 30 min for protonation of GCB. The protonated GCB beads were washed with distilled water to neutral pH, dried at room temperature and used for sorption studies.

2.6. Synthesis of Modified Biopolymers/TiO_2 nanocomposites:

Chitosan was prepared from the shrimp and crab shell by the chemical method. The synthesis of modified biopolymers/TiO2 nanocomposites was carried out by mixing titanium dioxide and carboxylated cross-linked chitosan beads (CCB) in the ratio 3:2 and the aqueous mixture was kept for 24 hr. The mixture was stirred well with 4g of polyvinyl alcohol at 70 ^oC for five hours. Then the mixture was calcined at 400 ^0C to get CCB/TiO_2 nanocomposites [38]. The same procedure was repeated for the synthesis of GCB/TiO_2 and PCB/TiO_2 nanocomposites by replacing the CCB with GCB and PCB biopolymers respectively.

2.7. Instrumental Studies:

The obtained samples, viz., CCB/TiO_2, PCB/TiO_2 and GCB/TiO_2 are characterized by using UV spectrophotometer, XRD analysis and SEM with EDAX analysis. The above analyses are carried out at Manonmaniam Sundaranar University, Tirunelveli, while the SEM with EDAX analysis are carried out at Karunya University at Coimbatore. The band gap energy value and particle sizes of the three samples are calculated by usual methods.

2.8. Defluoridation studies:

Defluoridation experiments were carried out by batch equilibration method in duplicate. In a typical case, 0.1 g of the sorbent was added to 100 ml of NaF solution of initial concentration 3 mg/L. The contents were shaken thoroughly using a thermostated shaker rotating at a speed of 200 rpm [39]. By keeping the mass of sorbent as 0.1 g and volume of solution as 100 ml at neutral pH. The solution was then filtered and the residual fluoride concentration was measured. The concentration of fluoride was measured using expandable ion analyzer EA 940 and the fluoride ion selective electrode BN 9609 (Orion, USA). The pH measurements were carried out with the same instrument with pH electrode. All other water quality parameters were analyzed by using standard methods.

Percentage of fluoride adsorption =

$$= \frac{(Fluoride\ adsorbed) \times 100}{3ppm}$$

3. Results and discussion

3.1. XRD Analysis

The obtained XRD pattern of chitosan is shown in Fig.1. The diffraction peaks appeared at diffraction angle 2θ= 11.9^o and 20.2^o are indicative of the high degree of

crystallinity morphology of chitosan [40], While there is a change in the peaks are observed in the XRD pattern of CCB/TiO_2, PCB/TiO_2 and GCB/TiO_2 nanocomposites. These are shown in figures.2a, 2b and 2c. The sharper and stronger peaks at 25.3°, 37.0° 37.8°, 38.6°, 48.0°, 53.9°, 55.1° and 62.7° were assigned to the (101), (103), (004), (112), (200), (105), (211) and (204) planes of distorted tetrahedral titanium dioxide, which can be indexed to the anatase - TiO_2 with high crystallinity. All the diffraction peaks are in good agreement with those of tetrahedral anatase structure of TiO_2 (JCPDS card 21-1272). Crystalline size was obtained by Debye – Scherrer formula. (Equation 1).

$$D=K\lambda/(\beta\cos\theta) \text{ ---------- (1)}$$

Where D is the crytal size; λ is the wavelength of the X-ray radiation (λ = 0.15406 nm) for CuKλ. K is usually taken as 0.89; and β is the line width at half – maximum height [41]. The crystallite size was calculated and the values 60.8 nm, 60.85 nm and 54 nm for GCB/TiO_2, CCB/TiO_2 and PCB/TiO_2 nanocomposites respectively.

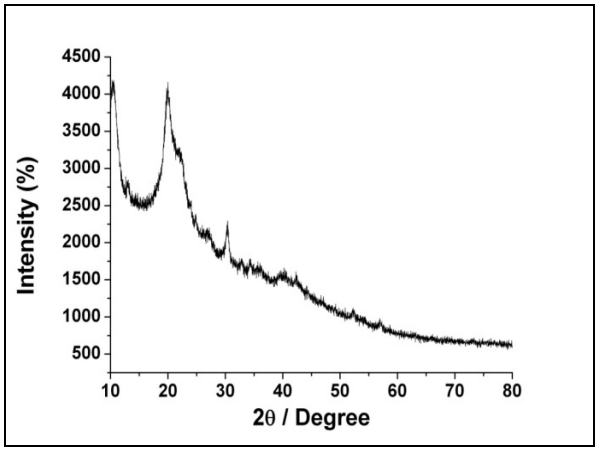

Fig 1: XRD pattern of Chitosan

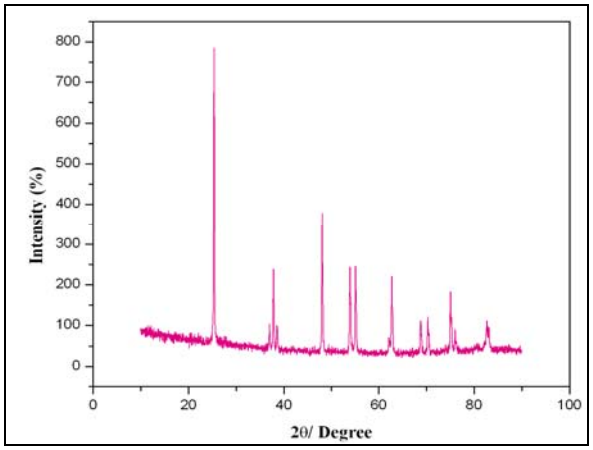

Fig 2: a.XRD pattern of CCB/TiO_2 nanocomposite

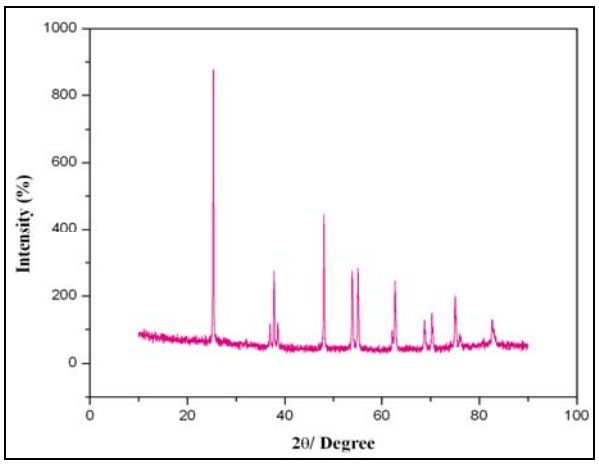

Fig 2: b.XRD pattern of PCB/TiO_2 nanocomposite

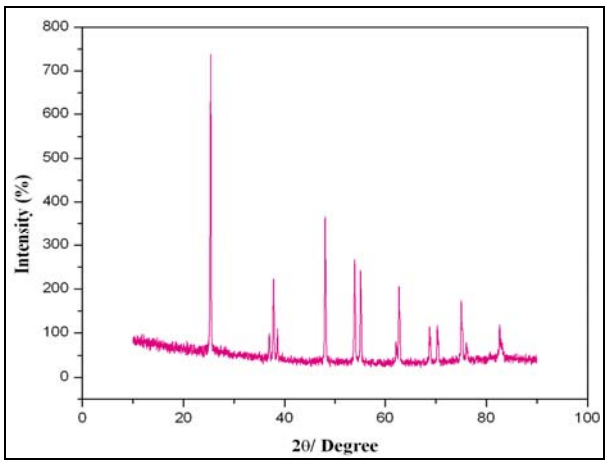

Fig 2: c. XRD pattern of GCB/TiO_2 nanocomposite

3.2. SEM analysis of Modified Biopolymers/TiO_2 nanocomposites:

SEM was used to investigate the surface morphology of modified biopolymers/TiO_2 nanocomposites. The figures (3a, 3b and 3c) show roughly spherical spongy shape and agglomeration of nanoparticles. The SEM image of the studied sample proved matrix consisting of micro sized chitosan derivative particles having layered structure with sub-micron particles of TiO_2 attached on the surface of the chitosan derivative matrix.

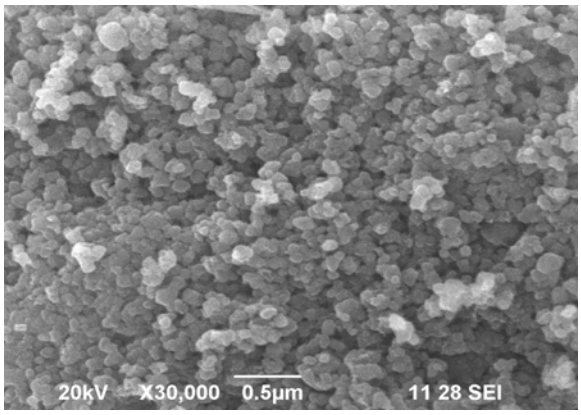

Fig 3: a. SEM image of CCB/TiO_2 nanocomposite

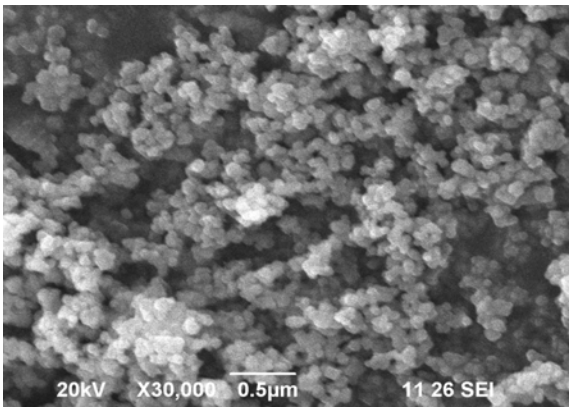

Fig 3: b. SEM image of PCB/TiO_2 nanocomposite

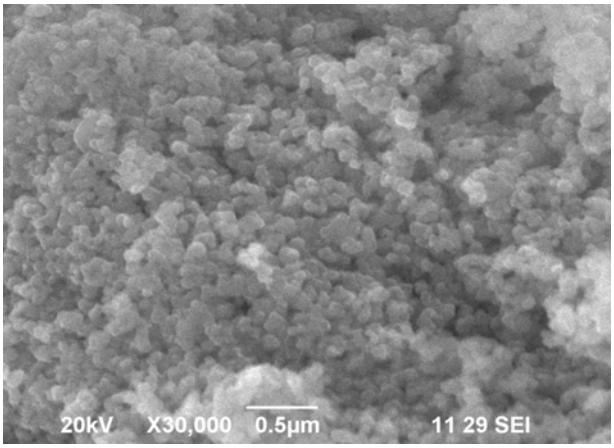

Fig 3: c. SEM image of GCB/TiO_2 nanocomposite

3.3. UV-Vis Absorption Spectroscopy analysis:

UV-Vis absorption spectrum is a useful absorption characterization to analyze nanomaterials. The UV-Vis spectral analysis was carried out between 200 nm and 800 nm. The pure TiO_2 nanomaterials were observed at 416 nm. The three samples were obtained at lower wavelength region. The absorption spectroscopy is very useful to calculate the optical band gap (Eg) with the help of the following equation.

$$\alpha = \frac{K(h\nu - E_g)^{n/2}}{h\nu} \text{ -------- (2)}$$

Where, $h\nu$ is the photon energy, α and n are constants. Where n is 2 for direct energy gap and ½ for an indirect energy gap.

The absorption edge is shifted to a higher energy (blue shift) and the corresponding band gap 3.6 eV for CCB/TiO_2 nanocomposites, 3.8 eV for PCB/TiO_2 nanocomposites and 3.4 eV for GCB/TiO_2 nanocomposites which are shown in Fig. 4a, 4b and 4c. The band gap energy values of obtained modified biopolymers/TiO_2 nanocomposites, which are higher than the value of 3.2 eV for the bulk TiO_2. This can be explained by the band gap of the semiconductor has been found to be particle size dependent [42]. Thus it is clear from the optical absorption study that the modified biopolymers/TiO_2 nanocomposites with different types of chitosan derivatives modifies the band gap of TiO_2 nanocomposites and the nanocomposites is blue shifted (higher energy) when compared with the bulk TiO_2. The blue shift might be caused by nanosize effect and structural defect of nanomaterials. Hence, the sample namely PCB/TiO_2 nanocomposite has high value of band gap energy.

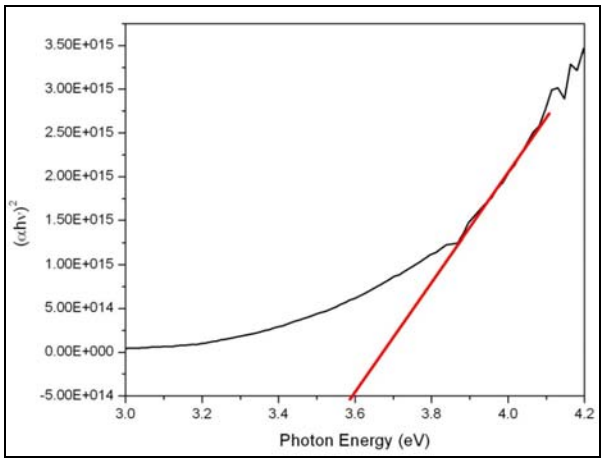

Fig 4: a. Band gap energy of CCB/TiO_2 nanocomposite

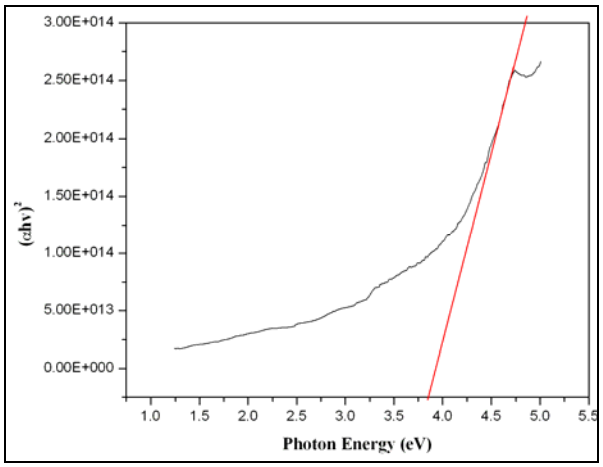

Fig 4: b. Band gap energy of PCB/TiO_2 nanocomposite

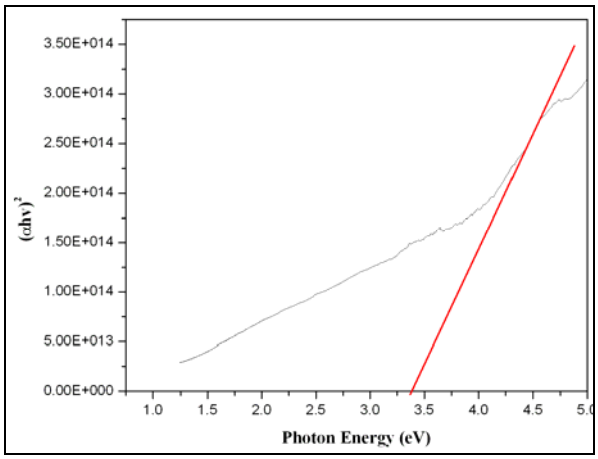

Fig 4: c. Band gap energy of GCB/TiO_2 nanocomposite

3. 4. Defluoridation studies using GCB/TiO_2, CCB/TiO_2 and PCB/TiO_2 nanocomposites:

3. 4.1. Effect of contact time:

The effect of DC of sorbents with contact time was studied using 3 mg/L as initial fluoride concentration with neutral pH at room temperature to find out the minimum time of contact needed to attain maximum DC. The sorption of fluoride has been investigated as a function of time in the range of 10–60 min. Fig. 5 shows the variation of DC of beads with time. It is evident from the graph that the DC of sorbents increases with increasing time and finally reaches saturation. Both sorbents reached saturation after 50 min to attain equilibrium. For subsequent experiments, 50 min was fixed as the contact time for all the sorbents. The percentage of fluoride removal for GCB/TiO_2, CCB/TiO_2 and PCB/TiO_2 nanocomposite is 86.33, 87.10 and 92.14 values are given in Table.1. respectively.

Table.1. Effect of Contat time

No	Time (min)	Percentage of fluoride removal (%)		
		GCB	CCB	PCB
1	10	62.84	63.51	65.12
2	20	66.20	67.25	70.14
3	30	70.65	73.40	74.18
4	40	72.81	74.12	80.92
5	50	86.33	87.10	92.14
6	60	86.33	87.10	92.14

Conc: 3ppm, pH: 7, Dose: 0.1g

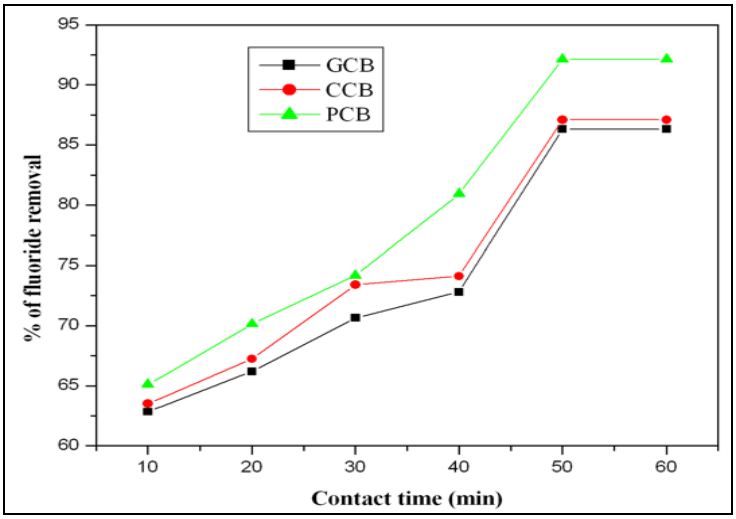

Fig 5: Effect of Contact time

3. 5. Instrumental studies:

3.5.1. Instrumental studies - XRD:

For understanding the nature of fluoride sorption on GCB/TiO_2, CCB/TiO_2 and PCB/TiO_2 nanocomposites were performed by using XRD analysis. The particle sizes of the above three nanocomposites were determined as 60.8 nm, 60.85 nm and 54 nm for GCB/TiO_2, CCB/TiO_2 and PCB/TiO_2 nanocomposites respectively. After the fluoride sorption, the XRD pattern of these samples were observed, where the sample PCB/TiO_2 is associated with major changes in the peaks. The XRD pattern of untreated nanocomposites and fluoride treated nanocomposites were shown in figures 6a and 6b, 7a and 7b and 8a and 8b. From the XRD pattern, we observed that the adsorption of fluoride on nanocomposites. The sample PCB/TiO_2 has maximum adsorption, due to lesser particle sizes and maximum band gap energy value.

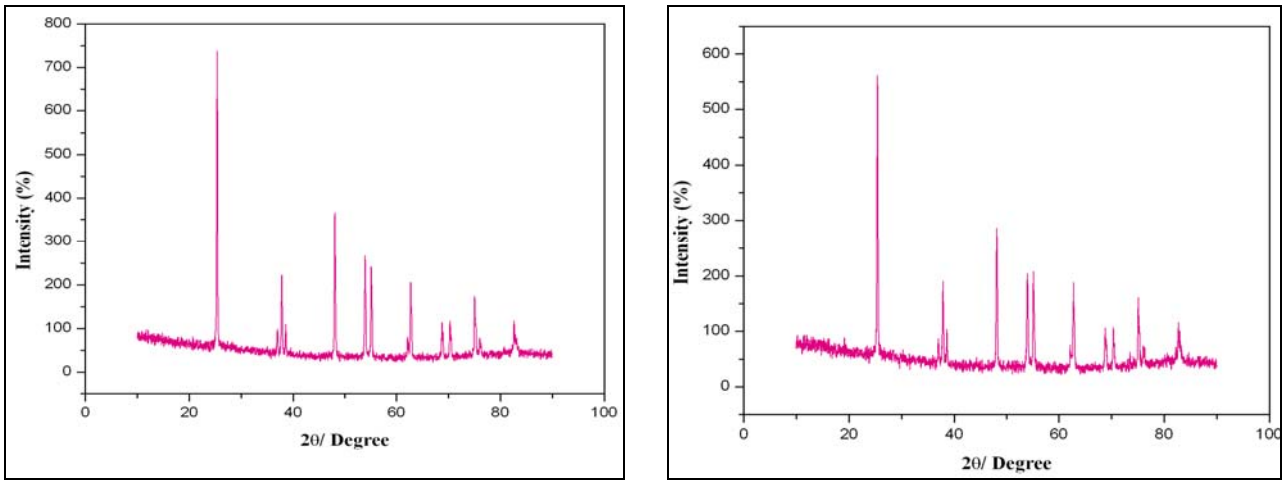

(a) **(b)**

Fig 6: a. XRD pattern of (a) GCB/TiO_2 nanocomposite and (b) fluoride treated GCB/TiO_2 nanocomposite

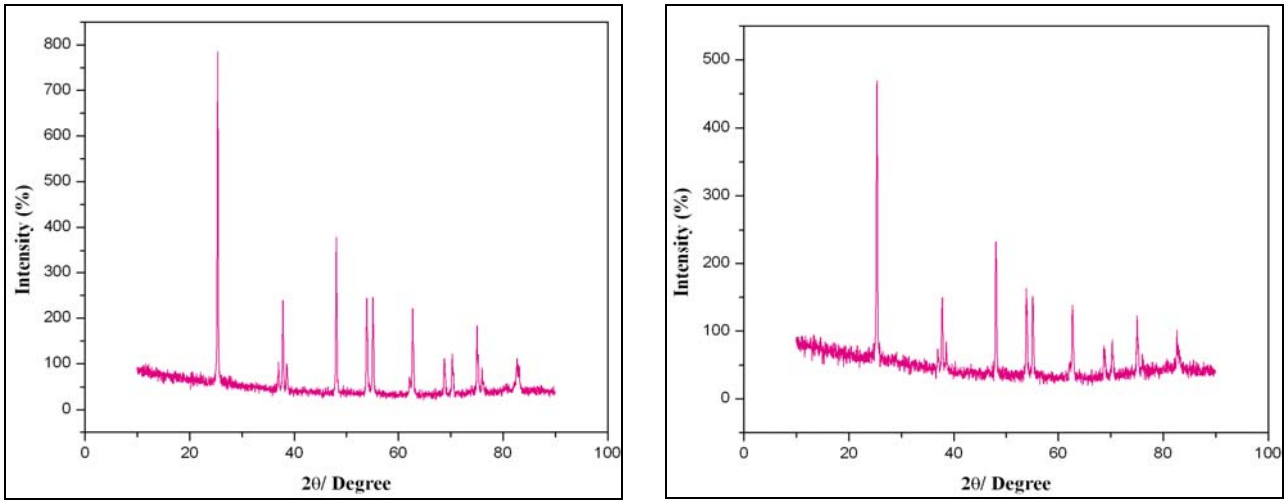

(a) **(b)**

Fig 7: a. XRD pattern of (a) CCB/TiO_2 nanocomposite and (b) fluoride treated CCB/TiO_2 nanocomposite

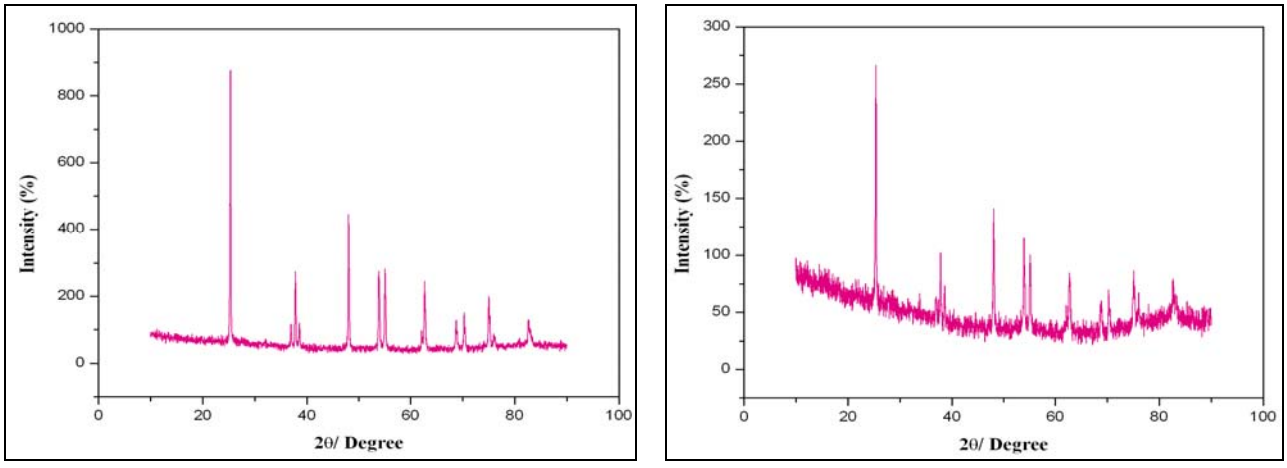

(a) **(b)**

Fig 8: a. XRD pattern of (a) PCB/TiO_2 nanocomposite and (b) fluoride treated PCB/TiO_2 nanocomposite

3.5.2. Instrumental studies – SEM with EDAX:

SEM was used to examine the surface morphology of the adsorbents. The SEM with EDAX spectra reveals that the presence of elements in the pure samples and fluoride treated samples. The change in the surface morphology of before and after fluoride treatment indicates fluoride adsorption on the nanocomposites. In the fluoride treated samples, a peak appears which is relevant to fluoride

element. This confirms that the fluoride sorption onto modified biopolymers/TiO_2 nanocomposites. The pure and fluoride treated SEM spectra and SEM with EDAX spectra are shown in figures 9a and 9b, 10a and 10b and 11a and 11b. Similarly 12a and 12b, 13a and 13b and 14a and 14b for GCB/TiO_2, CCB/TiO_2 and PCB/TiO_2 nanocomposites respectively. From the SEM analysis, PCB/TiO_2 nanocomposites shows that the best adsorbent for fluoride removal in water.

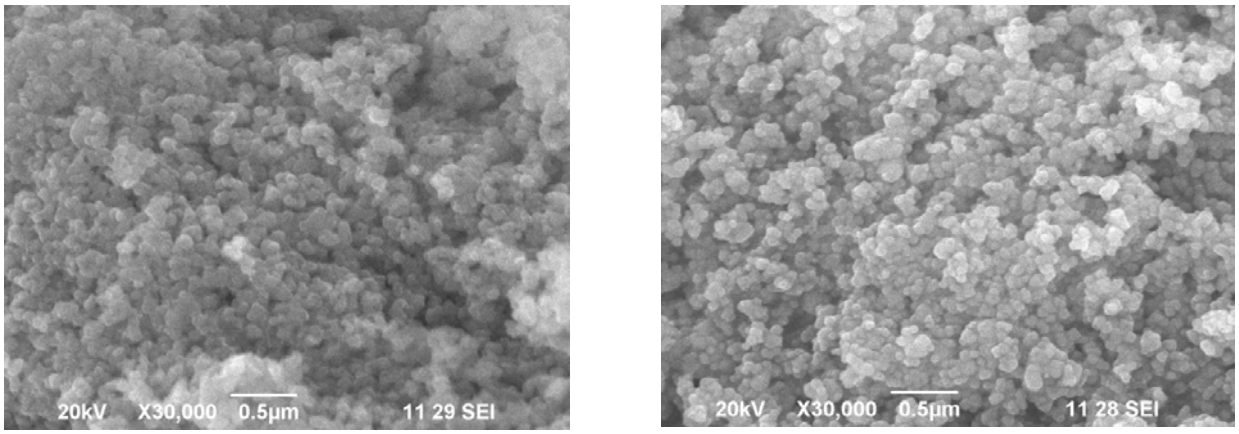

(a) **(b)**

Fig 9: a. SEM image of (a) GCB/TiO_2 nanocomposite and (b) fluoride treated GCB/TiO_2 nanocomposite

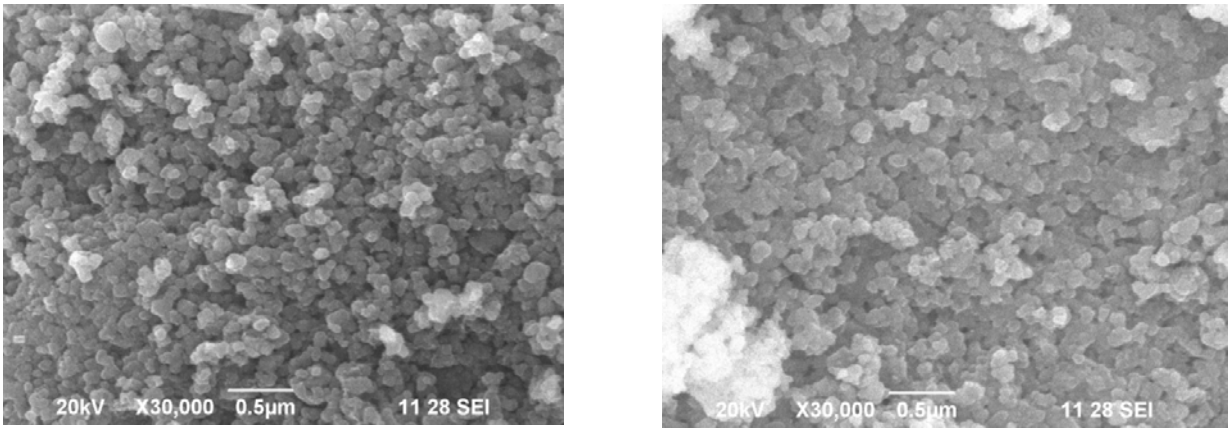

(a) **(b)**

Fig 10: a. SEM image of (a) CCB/TiO_2 nanocomposite and (b) fluoride treated CCB/TiO_2 nanocomposite

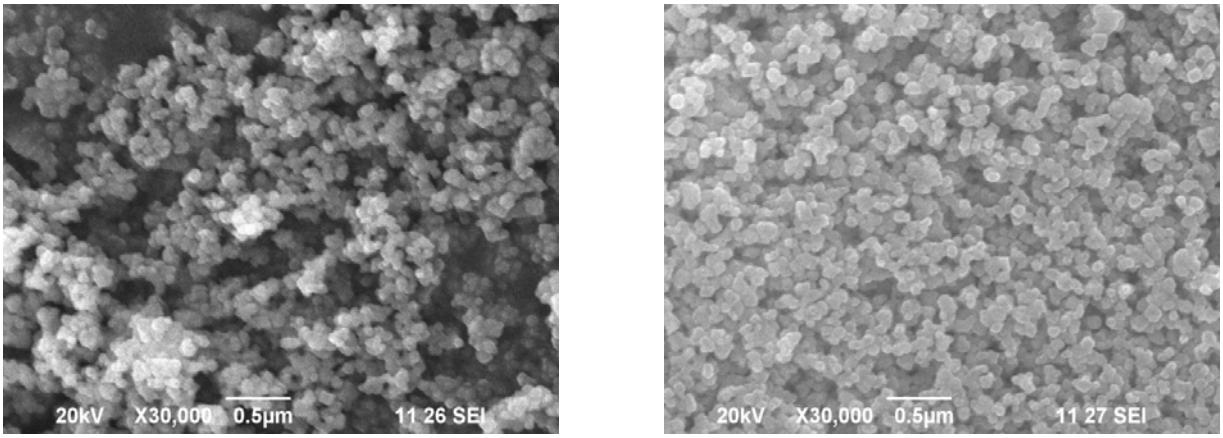

(a) **(b)**

Fig 11: a. SEM image of (a) PCB/TiO_2 nanocomposite and (b) fluoride treated PCB/TiO_2 nanocomposite

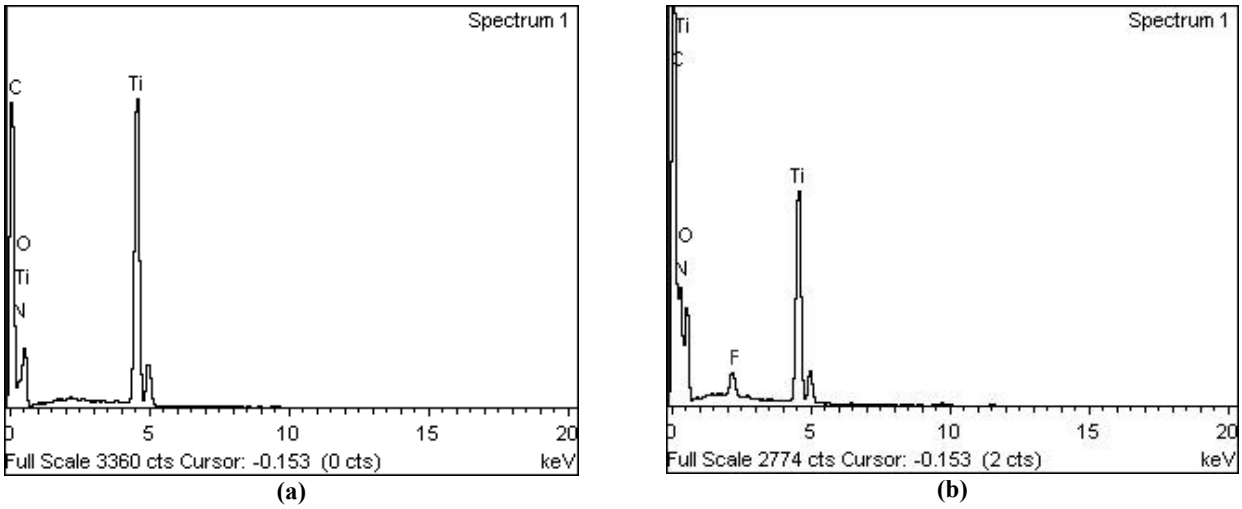

Fig 12: a. EDAX spectra of (a) GCB/TiO_2 nanocomposite and (b) fluoride treated GCB/TiO_2 nanocomposite

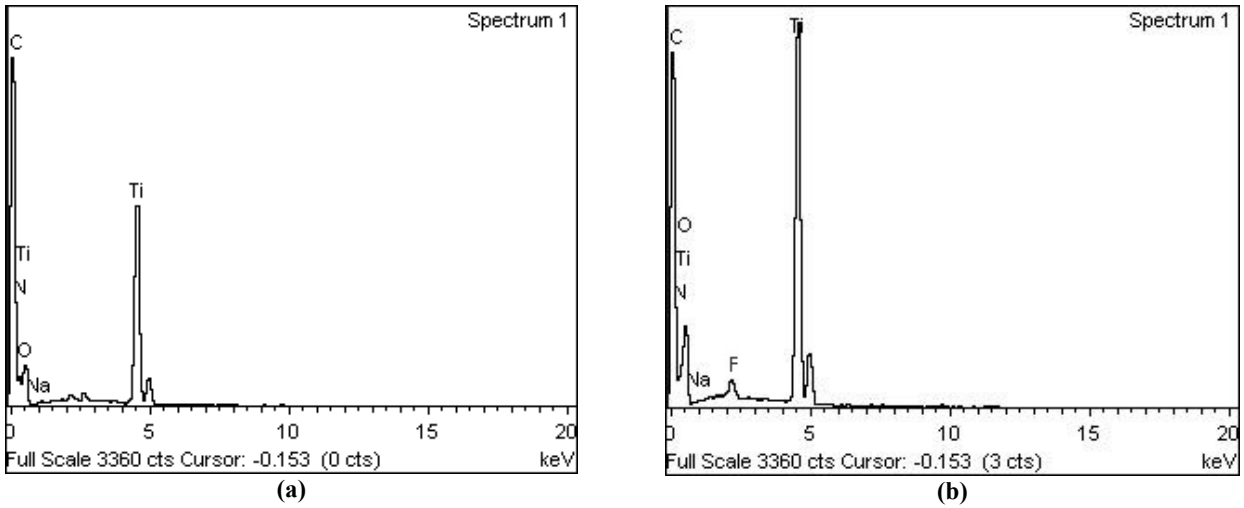

Fig 13: a. EDAX spectra of (a) CCB/TiO_2 nanocomposite and (b) fluoride treated CCB/TiO_2 nanocomposite

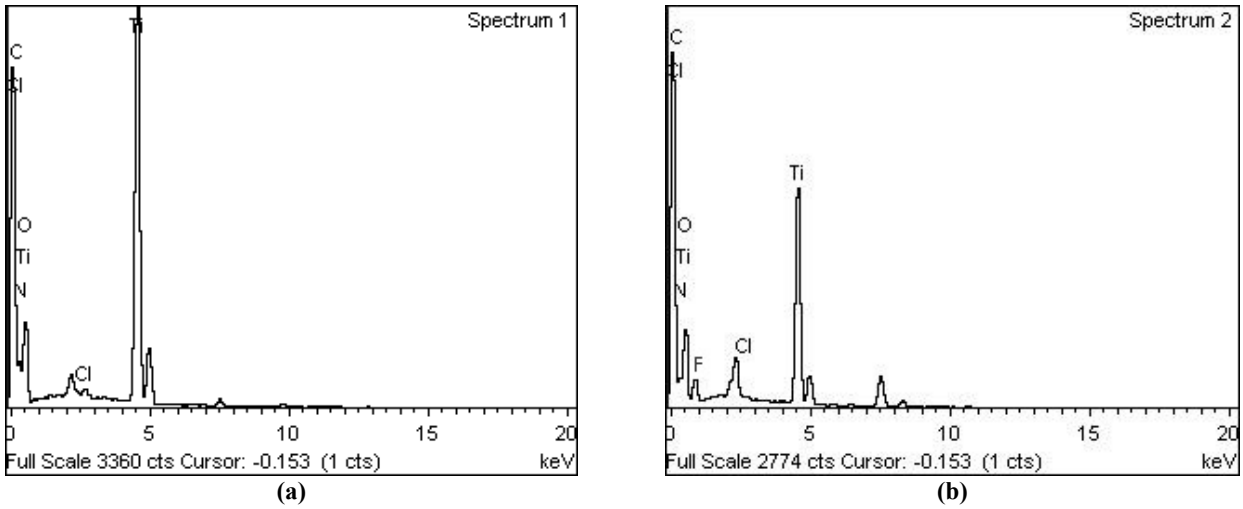

Fig 14: a. EDAX spectra of (a) PCB/TiO_2 nanocomposite and (b) fluoride treated d PCB/TiO_2 nanocomposite

4. Mechanism of adsorption

All the three modified biopolymers/TiO_2 nanocomposites remove fluoride by electrostatic attraction mechanism [43]. The modified form gets positively charged, due to the protonation of amino groups, which removes fluoride ion by means of electrostatic attraction. The possible mechanism of fluoride removal by PCB/TiO_2 is given in scheme 1. The presence of fluoride peak in the EDAX spectra of fluoride sorbed modified biopolymers/TiO_2 nanocomposites confirms the occurrence of fluoride sorption onto the nanocomposites (Fig. 14.a and 14.b).

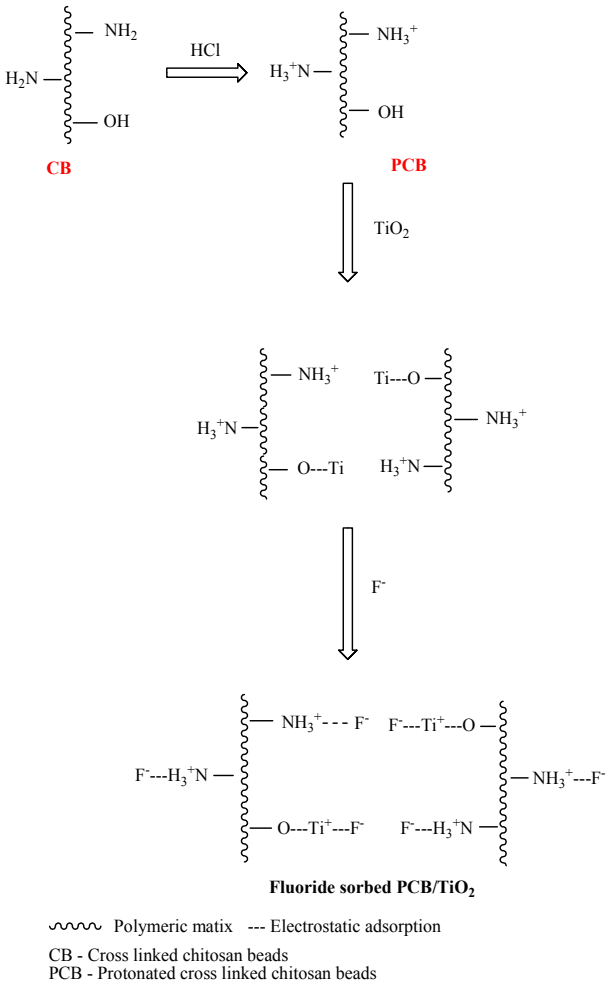

Scheme 1: Fluoride sorbed PCB/TiO_2 nanocomposites

5. Conclusion

In conclusion, the modified biopolymers/TiO_2 nanocomposites have been successfully synthesized by liquid phase technique. These materials are characterized using various analytical tools like XRD, SEM with EDAX and UV-vis absorption spectrum. An XRD result revealed the presence of distorted tetrahedral titanium dioxide, which can be indexed to the anatase-TiO_2 with high crystallinity. The average crystallite size of the sample was calculated using scherrer equation found to be 60.8 nm, 60.85 nm and 54 nm for GCB/TiO_2, CCB/TiO_2 and PCB/TiO_2 nanocomposites. SEM result shows spherical spongy shape and agglomeration of nanocomposites. Band gap energy of modified biopolymers/TiO_2 nanocomposites was found to 3.4 eV, 3.6 eV and 3.8 eV for GCB/TiO_2, CCB/TiO_2 and PCB/TiO_2 nanocomposites respectively, which is blue shifted (higher energy) compared with the bulk TiO_2. The nanocomposite was studied for the removal of fluoride ions from aqueous solution. The method is simple and has shown great potential for the removal of fluoride ions. PCB/TiO_2 has maximum percentage removal that is 92.14, which is higher than the others. Because of the particle size of PCB/TiO_2 is 54 nm, which is lower than the other nanocomposites. The mechanism of fluoride sorption of PCB/TiO_2 is governed by electrostatic adsorption. These modified chitosan beads/TiO_2 nanocomposites are stable and selective for fluoride sorption and could be used for field applications.

6. Reference

1. Reddy DR. Neurology of Endemic Skeletal Fluorosis. Neurology India. 2009; 57(1):7-12.
2. Jolly SS, Singh ID, Prasad S, Sharma R, Singh BM, Mathur OC. An Epidemiological Study of Endemic Fluorosis in Punjab. Indian Journal of Medical Research. 1969; 57(7):1333-1346.
3. Saravanan S, Kalyani C, Vijayarani M, Jayakodi P, Felix A, Nagarajan S. Prevalence of Dental Fluorosis among Primary Schoolchildren in Rural Areas of Chidambaram Taluk, Cuddalore District, Tamil Nadu. India. Indian Journal of Community Medicine. 2008; 33(3):146-150.
4. Shortt HE, Pandit CG, Raghvachari TNS. Endemic Fluorosis in Nellore District of South India. Indian Medical Gazettiar. 1937; 72:396-400.
5. Vijaya Y, Krishnaiah A, Column adsorption and desorption studies of fluoride on perchloric acid crosslinked calcium alginate beads. Eur. J. Chem. 2010; 7(1): 265–270.
6. Kumar JV, Moss ME, Fluorides in dental public health programs. Dent. Clin. North Am. 2008; 52(2): 387–401.
7. Ayoob S, Gupta AK, Fluoride in drinking water: A review on the status and stress effects, Environ. Sci. Technol. 2006; 36(6):433-487.
8. Sehn P, Fluoride removal with extra low energy reverse osmosis membranes: Three years of large scale field experience in Finland, Desalination. 2008; 223(1-3):73-84.
9. Dobaradaran S, Mahvi AH, Dehdashti S, Abadi DRV, Tehran I. Drinking water fluoride and child dental caries in Dashtestan, Iran. Fluoride. 2008; 41(3):220-226.
10. Huang CJ, Liu JC, Precipitate flotation of fluoride-containing wastewater from a semiconductor manufacturer. Water Res. 1999; 33 (16):3403-3412.
11. Yang M, Zhang Y, Shao B, Qi R, Myoga H. Precipitative removal of fluoride from electronics wastewater. J. Environ. Eng. 2001; 127(10):902-907.
12. Popat KM, Anand PS, Dasare BD. Selective removal of fluoride ions from water by the aluminium form of the aminomethylphosphonic acid-type ion exchanger. React. Polym. 1994; 23 (1):23-32.
13. Ku Y, Chiou HM, Wang W. The removal of fluoride ion from aqueous solution by a cation synthetic resin. Sep. Sci. Technol. 2002; 37(1):89-103.
14. Meeenakshi S, Viswanathan N. Identification of selective ion-exchange resin for fluoride sorption. J. Colloid Interface Sci. 2007; 308(2):438-450.
15. Karthikeyan G, Shanmuga Sundarraj A, Meenakshi S, Elango KP. Adsorption dynamics and the effect of temperature of fluoride at alumina-solution interface. J. Indian Chem.Soc. 2004; 81(6):461-466.
16. Ku Y, Chiou HM. The Adsorption of Fluoride Ion from Aqueous Solution by Activated Alumina. Water Air Soil Pollut. 2002; 133(1):349-361.
17. Amor Z, Bariou B, Mameri N, Taky M, Nicolas S, Elmidaoui A. Fluoride removal from brackish water by electrodialysis. Desalination. 2001; 133(3):215-223.
18. Daifullah AAM, Yakout SM, Elreefy SA. Adsorption of fluoride in aqueous solutions using $KMnO_4$-modified

activated carbon derived from steam pyrolysis of rice straw. J. Hazard. Mater. 2007; 147(1-2):633-643.
19. Tomar V, Kumar DA. critical study on efficiency of different materials for fluoride removal from aqueous media, Chem. Central J. 2013; 7(51):1-15.
20. Suriyaraj SP, Vijayaraghavan T, Biji P, Selvakumar R. Adsorption of fluoride from aqueous solution using different phases of microbially synthesized TiO_2 nanoparticles. J. Environ. Chem. Eng. 2014; 2(1):444-454.
21. Chauhan VS, Dwivedi PK, Iyengar L. Investigations on activated alumina based domestic defluoridation units. J. Hazard. Mater. 2007; 139(1):103-107.
22. Ayoob S, Gupta AK. Insights into isotherm making in the sorptive removal of fluoride from drinking water. J. Hazard. Mater. 2008; 152(3):976-985.
23. Yadav AK, Kaushik CP, Haritash AK, Kansal A. Rani N, Defluoridation of groundwater using brick powder as an adsorbent. J. Hazard. Mater. 2006; 128(2-3):289-293.
24. Mahramanlioglu M, Kizilcikli I, Bicer IO. Adsorption of fluoride from aqueous solution by acid treated spent bleaching earth. J. Fluorine Chem. 2002; 115(1):41-47.
25. Dayananda D, Sarva VR, Prasad SV, Arunachalam J, Ghosh NN. Preparation of CaO loaded mesoporous Al2O3: Efficient adsorbent for fluoride removal from water, Chem. Eng. J. 2014; 248:430-439.
26. Kafedjiiski K, Kurniawan AH, Hoffer MH, Schnurch AB. Synthesis and in vitro evaluation of a novel thiolated chitosan. Biomaterials 2005; 26(7):819-826.
27. Jayakumar R, Prabaharan M, Reis RL, Mano JF. Graft copolymerized chitosan-present status and applications. Carbohydr. Polym. 2005; 62(2):142-158.
28. Jayakumar R, Reis RL, Mano JF, Chemistry and Applications of Phosphorylated Chitin and Chitosan. E-Polymer. 2006; 6(1):1-16.
29. Jayakumar R, New N, Tokura S, Tamura H, ulfated chitin and chitosan as novel biomaterials. Int. J. Biol. Macromol. 2007; 40(3):175-181.
30. Juang RS, Shao HJ A. simplified equilibrium model for sorption of heavy metal ions from aqueous solutions on chitosan. Water Res. 2002; 36(12):2999-3008.
31. Jayakumar R, Rajkumar M, Freitas H, Selvamurugan N, Nair SV, Furuike T. Preparation, characterization, bioactive and metal uptake studies of alginate/phosphorylated chitin blend films. Int. J. Biol. Macromol. 2009; 44(1):107-111.
32. Sag Y, Aytay Y. Kinetic studies on sorption of Cr (VI) and Cu (II) ions by chitin, chitosan and *Rhizopus arrhizus*. Biochem. Eng. J. 2002; 12(2):143-153.
33. Yang TC, Zall RR. Absorption of metals by natural polymers generated from seafood processing wastes. Ind. Eng. Chem. Prod. Res. Dev. 1984; 23(1):168-172.
34. Jeon C, Holl WH, Chemical modification of chitosan and equilibrium study for mercury ion removal. Water Res. 2003; 37(19):4770-4780.
35. Jaafari K, Elmaleh S, Coma J, Benkhouja K. Equilibrium and kinetics of nitrate removal by protonated cross-linked chitosan. Water SA. 2001; 27(1):9-14.
36. Viswanathan N, Sairam Sundaram C, Meenakshi S. Removal of fluoride from aqueous solution using protonated chitosan beads. J. Hazard. Mater. 2009; 161(1):423-430.
37. Viswanathan N, Sairam Sundaram C, Meenakshi S. Sorption behaviour of fluoride on carboxylated cross-linked chitosan beads. Colloid Surf. B. 2009; 68(1):48-54.
38. Sairam Sundaram C, Natrayasamy Viswanathan, Meenakshi S. Defluoridation of water using magnesia/chitosan composite. Journal of Hazardous Materials. 2009; 163(2-3):618-624.
39. Kousalya GN, Muniyappan Rajiv Gandhi, Meenakshi S. Sorption of chromium (VI) using modified forms of chitosan beads. International Journal of Biological Macromolecules. 2010; 47(2):308-315.
40. Abdeen Z, Mohammed SG. Study of the Adsorption Efficiency of an Eco-Friendly Carbohydrate Polymer for Contaminated Aqueous Solution by Organophosphorus pesticides. Ojopm. 2014; 4:16-28.
41. Qiu S, Kalita SJ. Synthesis, processing and characterization of nanocrystalline titanium dioxide. Materials science and Engineering A. 2006; 435-436(5):327-332.
42. Coma A, Misfud A, Sanz E. Kinetics of the acid leaching of palygorskite: influence of the octahedral sheet composition, Clay miner. 1990; 25:197-205.
43. Rojas G, Silva J, Flores JA, Rodriguez A, Ly M, Maldonado H. Adsorption of chromium onto cross-linked chitosan. Sep. Purif. Technol. 2005; 44(1):31-36.